PHYSICSAccess Research Paper
ISSN Online: 2756-3898, ISSN Print: 2714-500X https://doi.org/10.47514/phyaccess.2026.6.1.012

Exploring Intermediate and Natural Inflation under a Nonminimal Derivative Coupling: The John-George Framework

Ferdinand Mavoa[1, 2], Mohamed C Sow[1], Hoavo Hova[3], Moussiliou G Ganiou[4], Cheikh S Touré[1], and Antonin D Kanfon[5]

[1] Département Énergie Photovoltaïque, Université de Labé, BP: (+224) 2010, Labé, République de Guinée
[2] 1International Chair of Mathematical Physics and Application (ICMPA), Université d'Abomey-Calavi, 072 BP 50, Cotonou, Bénin
[3] Département de Physique, Faculté des Sciences, Université de Kara, BP: 404 Kara, République du Togo
[4] Département de Physique, Université Gamal Abdel Nasser, BP 1147 Conakry, République de Guinée
[5] Université Nationale des Sciences Informatique et Mathématiques, BP 486 Abomey, République du Bénin

Corresponding E-mail: maferdson@yahoo.fr

Received 21-02-2026
Accepted for publication 29-04-2026
Published 14-05-2026

Abstract

Intermediate and natural inflation are investigated within a nonminimal derivative coupling scalar field model, namely the John–George framework. The derivative coupling introduces enhanced gravitational friction, modifying inflaton dynamics and enabling sustained accelerated expansion even for sub-Planckian parameter values. The field equations and slow-roll parameters are derived in a flat Friedmann–Lemaître–Robertson–Walker spacetime. For intermediate inflation, the effective potential is reconstructed assuming a power-law scalar field evolution, while a periodic potential with a decay constant, f describes the natural inflation. Numerical analysis of inflationary observables yields $n_s = 0.96397$ and $r = 0.0019$ for intermediate inflation, and $n_s = 0.961176$ and $r = 0.00651$ for natural inflation at $N = 60$e-folds. These predictions are in excellent agreement with Planck and BICEP/Keck constraints. The enhanced friction mechanism slows the inflaton evolution and suppresses the tensor-to-scalar ratio, bringing the model well within observational bounds. Parameter analysis indicates that $m \approx 0.5$–1 and $f \approx 0.5$ provide optimal agreement with data. The John–George framework, therefore, constitutes a viable and competitive alternative to standard inflationary scenarios.

Keywords: Nonminimal derivative coupling; Intermediate inflation; Natural inflation; Cosmological perturbation; John and George models.

I. Introduction

To solve the problems generated by the standard Big Bang cosmology, such as the problems of the Horizon and flatness, an inflationary era was proposed at the beginning of the Early Universe. The success of the inflation paradigm could make it possible to establish a causal mechanism that

generates the primordial density of perturbations necessary for the formation of the large structures in the Universe [1–5]. The simple inflationary scenario with a single scalar field called inflation predicted that the dominant mode of primordial density fluctuations is highly adiabatic, scale-invariant, and Gaussian [6]. Several studies have been conducted in this framework of cosmological inflation with a field and have given interesting results [7–8]. But recent observational data have detected a level of scale dependence in the primordial perturbations [9–10]. Several proposed inflationary models give information based on the theories they support. Thus, it has been shown that a significant amount of very important information about the dynamics of the initial inflationary expansion of the Universe can be found in primordial scalar non-Gaussianities [11]. Therefore, the models of extended inflation, which can show the non-Gaussianity and scale dependence of the primordial perturbation, are very favorable. Among the extended inflationary models that have really received special attention from the scientific community is the non-minimal coupling whose scalar field function is related to the Ricci constant in the form $f(\phi)R$. The information to which this extended inflationary model has paid particular attention is set out in [10].

A generalized inflationary model in which the potential $V(\phi)$ is coupled to the curvature and an extension of the nonminimal derivative term in the Lagrangian as $\frac{1}{2}(g^{\mu\nu} + \gamma\kappa G^{\mu\nu})\nabla_\mu\phi\nabla_\nu\phi$ was considered in this study. This type of extended inflationary model is called the John and George model, developed in [12−13]. Several studies have also discussed a special case of non-minimal coupling of the scalar field called non-minimally derivative coupling. This type of coupling gives higher than second-order derivatives in field equations, and more degrees of freedom [14−16]. Note that Nonminimal Derivative Coupling is a subset of Horndeski's theory that satisfies the necessary conditions to be theoretically a good inflationary model. The main properties of the cosmological perturbations are described by the tensor-to-scalar ratio and the scalar spectral index. The Planck temperature and polarization data on the measurements of the cosmic microwave background anisotropies give $n_s = 0.9649 \pm 0.0042$ and $r < 0.056$ [17].

This study focuses on intermediate inflation characterized by a scale factor of the form $a = a_0 e^{At^\lambda}$, where $A > 0$and $0 < \lambda < 1$[18–20]. The resulting cosmic expansion is slower than that of de Sitter inflation $(a(t) \propto \exp(Ht))$, where H is constant, but faster than power-law inflation $(a(t) \propto t^q, q > 1)$ [21]. Intermediate inflation has been extensively studied within the standard inflationary framework [18–21], while inflation driven by a natural potential has also been widely investigated with notable success [22–24]. In natural inflation, a pseudo–Nambu–Goldstone boson acts as the inflaton, with a cosine potential arising from non-perturbative effects. This model, in its original formulation, is strongly constrained by recent Planck Collaboration–BICEP/Keck Collaboration observations [5], and the parameter region most consistent with cosmic microwave background measurements (CMB) typically corresponds to trans-Planckian values of the axion decay constant [25].

Within this context, intermediate and natural inflation are investigated using the John and George model. The Friedmann equations and the corresponding equations of motion are derived from the model action, followed by the application of the slow-roll approximation. The intermediate inflationary potential is constructed and used to determine the associated inflationary parameters. In addition, the natural inflation potential, as established in the literature, is employed to evaluate the corresponding parameters. A numerical analysis is performed, and the results are compared with observational data. The study is further extended to include the analysis of cosmological perturbations associated with the inflationary dynamics of the model.

II. Model Presentation

Natural units were adopted in this study, where the reduced Planck mass is defined as $M_p = (8\pi G)^{-1/2}$. Unless otherwise stated, $M_p = 1$ was set for convenience, and the metric signature $(-,+,+,+)$ was used alongside the standard conventions for curvature tensors.

The model considered in this work corresponds to the so-called John–George sector of Horndeski gravity, which introduces a nonminimal derivative coupling between the scalar field and the Einstein tensor. This coupling modifies the kinetic structure of the scalar field and generates an enhanced gravitational friction during inflation.

The parameters γ and ϵ are dimensionless coupling constants. The parameter γ controls the strength of the derivative coupling between the scalar field and the Einstein tensor $G^{\mu\nu}$, while ϵ determines the coupling between the scalar potential and the curvature sector. In the limit $\gamma \to 0$ and $\epsilon \to 0$, the model reduces to the standard minimally coupled scalar field theory.

The action of the John-George models is as follows:

$$S = \int \sqrt{-g}\left[\frac{M_p^2}{2}(1 + \epsilon V(\phi))\frac{R}{2k} - \frac{1}{2}(g^{\mu\nu} + \gamma k G^{\mu\nu})\nabla_\mu\phi\nabla_\nu\phi\right]d^4x \quad (1)$$

Where $\kappa = \frac{1}{M_p^2}$, γ and ϵ are dimensionless parameters. This action corresponds to a specific sector of Horndeski theory [26], for conditions described in [13].

Varying the action with respect to the metric $g_{\mu\nu}$ leads to the modified Einstein field equations.

$$\frac{M_p^2}{2k}(1 + \epsilon V(\phi))G_{\mu\nu} = T^{\phi}_{\mu\nu} + \gamma k\Theta_{\mu\nu} + \frac{M_p^2}{2\kappa}\epsilon\left[g_{\mu\nu}\Box V(\phi) - \nabla_\mu\nabla_\nu V(\phi)\right] \quad (2)$$

The standard energy-momentum tensor of the scalar field is given by:

$$T^{\phi}_{\mu\nu} = \nabla_\mu\phi\nabla_\nu\phi - \frac{1}{2}g_{\mu\nu}(\nabla\phi)^2 \quad (3)$$

The contribution arising from the nonminimal derivative

coupling reads:

$$\Theta_{\mu\nu} = -\frac{1}{2}\nabla_\mu\phi\nabla_\nu\phi R + 2\nabla_\alpha\phi\nabla_{(\mu}\phi R^{\alpha}_{\nu)} + \nabla^\alpha\phi\nabla^\beta\phi R_{\mu\alpha\nu\beta} + \nabla_\mu\nabla^\alpha\phi\nabla_\nu\nabla_\alpha\phi - \nabla_\mu\nabla_\nu\phi\phi - \frac{1}{2}g_{\mu\nu}[(\nabla\nabla\phi)^2 - (\Box\phi)^2] \quad (4)$$

Assuming a spatially flat Friedmann–Robertson–Walker (FRW) spacetime, the modified Friedmann equations are obtained as follows.

The first Friedmann equation takes the form:

$$3H^2(1+\epsilon V(\phi)) = \frac{1}{2}\dot{\phi}^2 + 9\gamma H^2\dot{\phi}^2 + 3\epsilon H\dot{\phi}V'(\phi) \quad (5)$$

The second Friedmann equation is given by:

$$\left(2\dot{H}+3H^2\right)\left(1+\epsilon V(\phi)\right) + \epsilon V'(\phi)\left(\ddot{\phi}+2H\dot{\phi}\right) + \frac{\kappa\dot{\phi}^2}{2}\Big[1 + \gamma\kappa\left(3H^2+2\dot{H}+4H\frac{\ddot{\phi}}{\dot{\phi}}\right)\Big] + \epsilon\dot{\phi}^2V''(\phi) = 0 \quad (6)$$

Finally, variation of the action with respect to the scalar field ϕ leads to the modified Klein–Gordon equation.

$$(1+3\gamma H^2)\ddot{\phi} + 3H(1+3\gamma H^2+2\gamma\dot{H})\dot{\phi} + \frac{M_p^2}{4\kappa}\epsilon V'(\phi)R = 0 \quad (7)$$

A. Slow-roll approximation

Under the slow-roll approximation, the second derivative of the scalar field and the time variation of the Hubble parameter are assumed to be negligible, i.e. $\ddot{\phi} \ll H\dot{\phi}$ and $|\dot{H}| \ll H^2$. The Klein–Gordon equation then reduces to

$$3H(1+3\gamma H^2)\dot{\phi} + \frac{M_p^2}{4\kappa}\epsilon V'(\phi)R \simeq 0 \quad (8)$$

In a spatially flat Friedmann–Robertson–Walker background, the Ricci scalar is given by

$$R = 6(2H^2+\dot{H}) \quad (9)$$

Using the slow-roll condition $|\dot{H}| \ll H^2$, (9) simplifies to (10).

$$R \simeq 12H^2 \quad (10)$$

Substituting this result into the Klein–Gordon equation gives (11).

$$3H(1+3\gamma H^2)\dot{\phi} + \frac{3M_p^2}{\kappa}\epsilon H^2V'(\phi) \simeq 0 \quad (11)$$

Finally, solving for $\dot{\phi}$ yields

$$\dot{\phi} \simeq -\frac{M_p^2}{\kappa}\frac{\epsilon H}{(1+3\gamma H^2)}V'(\phi) \quad (12)$$

The derivative coupling enhances the effective friction acting on the scalar field, which allows slow-roll inflation to occur even for steeper potentials. This mechanism plays an important role in reducing the tensor-to-scalar ratio predicted by the model.

The slow-roll approximation is implemented by neglecting the second derivative of the scalar field ($\ddot{\phi} \ll H\dot{\phi}$) and assuming a quasi-de Sitter expansion ($|\dot{H}| \ll H^2$). In addition, the kinetic energy of the scalar field is assumed to be subdominant compared to the potential energy ($\dot{\phi}^2 \ll V(\phi)$).

In the presence of nonminimal derivative coupling, the scalar field equation contains an effective friction term proportional to $(1+3\gamma H^2)$. Two regimes can be identified: for $\gamma H^2 \ll 1$, the model reduces to the standard slow-roll inflation, whereas for $\gamma H^2 \gg 1$ the derivative coupling dominates the dynamics. In the high-friction regime, the effective damping term is significantly enhanced, leading to a suppression of $\dot{\phi}$ and ensuring that the slow-roll conditions remain valid even for steep potentials. To further support the validity of the slow-roll approximation, it was numerically verified that the conditions $\ddot{\phi}/(H\dot{\phi}) \ll 1$ and $\dot{\phi}^2/V \ll 1$ are satisfied throughout the inflationary evolution.

III. Intermediate Inflation with John - George Model

Here, the interest is in intermediate inflation, which is one of the interesting scenarios of inflationary models. In intermediate inflation, the scale factor evolves faster than a power law ($a = t^p$) inflation but slower than standard de Sitter inflation ($a = \exp(Ht)$) [27]. Additionally, the intermediate inflation is specified by the scale factor given by (13).

$$a = a_O\exp(At^\lambda) \quad (13)$$

Where $A > 0$ and $0 < \lambda < 1$ are two constants [28]. This form describes an expansion rate that is slower than exponential inflation but faster than power-law inflation. Thus, the Hubble parameter is as in (14).

$$H = \frac{\dot{a}}{a} = \lambda At^{\lambda-1} \quad (14)$$

Following the reconstruction method described in [28], a power-law evolution for the scalar field was assumed, given by (15).

$$\phi(t) = Ct^m \quad (15)$$

This choice should be interpreted as a reconstruction method that allows the potential $V(\phi)$ to be determined from the background dynamics. Within the slow-roll regime, the resulting potential remains positive and well behaved during the inflationary phase.

The prime derivative of $\phi(t)$ with respect to the given time

$$\dot{\phi}(t) = mCt^{m-1} \quad (16)$$

with C and m constants.

Reference (5) takes the form given by (17) during the inflationary period and in the slow-roll approximation, where $\dot{\phi}^2 \ll V(\phi)$ and $\ddot{\phi} \ll 3H\dot{\phi}$.

$$3H^2(1+\epsilon V(\phi)) + 3\epsilon H\dot{\phi}V'(\phi) = 0 \quad (17)$$

Using (14), (15), and (16) in (17), and after integration, the intermediate potential result of the John and George model was obtained, as given by (18).

$$V(\phi) = \frac{1}{\epsilon}\left[-1 + K\exp\left(\frac{\lambda A}{m(\lambda-m)}\left(\frac{1}{C}\right)^{\frac{\lambda+1}{m}}\phi^{\frac{\lambda-m+1}{m}}\right)\right] \quad (18)$$

Where K is the integration constant.

A. Clarification on the reconstruction of the intermediate inflation potential

The choice of the intermediate form of the scale factor, together with a power-law evolution of the scalar field, is adopted within the framework of a reconstruction approach. In this context, the aim is not to derive the dynamics from first principles, but rather to determine the form of the scalar field potential that can reproduce a desired cosmological evolution.

Therefore, the assumed behavior does not correspond to an exact attractor solution. Instead, it should be interpreted as an effective description of the inflationary dynamics, where the

expansion history is specified in advance, and the corresponding scalar field model is reconstructed accordingly. This method is widely used in inflationary cosmology, as it allows one to explore viable models capable of generating specific expansion scenarios consistent with observations.

At the same time, the adopted evolution of the scalar field can be seen as a reasonable approximation of a slow-roll trajectory. During the inflationary phase, the scalar field is expected to evolve smoothly and gradually, and a power-law behavior provides a simple yet effective way to capture this feature.

Regarding the physical viability of the reconstructed potential, it remains positive and well-behaved over the entire inflationary regime for suitable choices of the model parameters. The potential evolves smoothly without pathological features, ensuring a stable inflationary phase. This regular behavior supports the consistency of the model and its ability to describe a realistic inflationary scenario.

In summary, the adopted ansatz should be understood as a reconstruction scheme designed to reproduce an intermediate inflationary expansion, while maintaining physical consistency and compatibility with the general expectations of slow-roll inflation.

Fig. 1 shows the evolution of the intermediate potential $V(\phi)$ as a function of the scalar field ϕ. It can be seen that $V(\phi)$ grows with respect to ϕ.

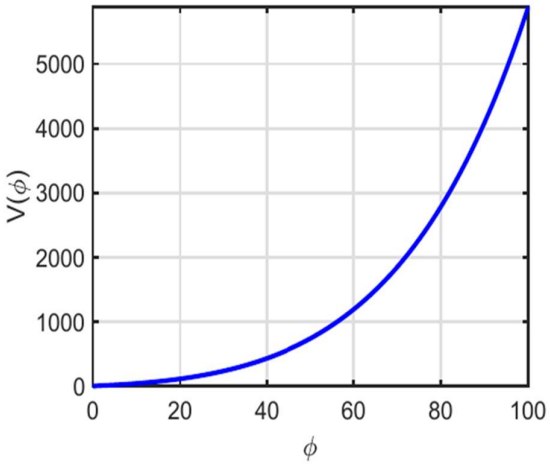

Fig. 1. Evolution of potential $V(\emptyset)$ versus scalar field $\emptyset$ for $\in = 0.2; m = 0.2; K = 1;\ \lambda = 0.2; C = 0.2; A = 0.2.$

Furthermore, the slow-roll parameters are defined as follows:

$$\varepsilon = -\frac{\dot{H}}{H^2} \tag{19}$$

$$\eta = -\frac{\ddot{H}}{\dot{H}H} \tag{20}$$

Note that inflation is achieved when $\varepsilon < 1$, $\eta < 1$ and ends when the slow-roll parameters reach unity [29].

Equations (17), (21), and (22) give (21), (22), and (23) respectively:

$$\varepsilon = \left(\frac{1+\epsilon V(\phi)}{\epsilon V'(\phi)}\right)\left(\epsilon^2 V'^2(\phi) - (1+\epsilon V(\phi))V''(\phi)\right) \tag{21}$$

$$\eta = \frac{2\epsilon^2 V''(\phi)(1+\epsilon V(\phi)) + \epsilon^3 V'(\phi) - V'''(\phi)(1+\epsilon V(\phi))^2}{\epsilon^2(V''(\phi) - \epsilon^2 V'^2(\phi))} \tag{22}$$

and the e-fold number is,

$$N = \int_{t_i}^{t_f} H\, dt \tag{23}$$

Where t_f and t_i are respectively the end and the beginning of the inflation.

Equation (23) can be put in the form of (24).

$$N \approx \int_{\phi_{hc}}^{\phi_f} \frac{H}{\dot{\phi}} d\phi \tag{24}$$

Using (17), (24) becomes (25).

$$N = -\int_{\phi_{hc}}^{\phi_f} \frac{\epsilon V'(\phi)}{1+\epsilon V(\phi)} d\phi \tag{25}$$

Where ϕ_{hc} and ϕ_f are respectively the values of ϕ when the universe scale observed today crosses the Hubble horizon during inflation, and when the universe exits the inflationary phase.

Using (18) in (25) gives (26).

$$N = -\frac{\lambda A}{mC(\lambda+1-m)}\left(\frac{1}{C}\right)^{\frac{\lambda-m+1}{m}}\left[\phi_f^{\frac{\lambda-m+1}{m}} - \phi_{hc}^{\frac{\lambda-m+1}{m}}\right] \tag{26}$$

Using the same potential (18), (21), and (22), give rise to (27) and (28) respectively.

$$\varepsilon = K\left[\frac{\lambda A(\epsilon-1)+C^{\frac{\lambda+1}{m}} m(\lambda-2m+1)}{\lambda A}\phi^{\frac{-\lambda-1+2m}{m}}\right]\exp(Z\phi^P) \tag{27}$$

$$\eta = \frac{2\epsilon K\left[\frac{-2m+\lambda+1}{m}+\frac{\lambda A}{m^2}\left(\frac{1}{C}\right)^{\frac{\lambda+1}{m}}\phi^{\frac{\lambda-2m+1}{m}}\right]\exp(Z\phi^P)}{K\epsilon\left(\frac{-2m+\lambda+1}{m}+\frac{\lambda A}{m^2}\left(\frac{1}{C}\right)^{\frac{\lambda+1}{m}}\phi^{\frac{\lambda-2m+1}{m}}\right)-\epsilon^4\frac{\lambda A}{m^2}\left(\frac{1}{C}\right)^{\frac{\lambda+1}{m}}\exp(Z\phi^P)} + \frac{\left[\left(\epsilon^3\frac{\lambda A}{m^2}\left(\frac{1}{C}\right)^{\frac{\lambda+1}{m}}\right)^2 - \frac{K^3}{\epsilon}\left(\frac{-2m+\lambda+1}{m}\phi^{-1}+\left(\frac{1}{C}\right)^{\frac{\lambda+1}{m}}\phi^{\frac{\lambda-2m+1}{m}}\right)\right]\exp(2Z\phi^P)}{K\epsilon\left(\frac{-2m+\lambda+1}{m}+\frac{\lambda A}{m^2}\left(\frac{1}{C}\right)^{\frac{\lambda+1}{m}}\phi^{\frac{\lambda-2m+1}{m}}\right)-\epsilon^4\frac{\lambda A}{m^2}\left(\frac{1}{C}\right)^{\frac{\lambda+1}{m}}\exp(Z\phi^P)} \tag{28}$$

With,

$$Z = \frac{\lambda A}{m(\lambda+1-m)}\left(\frac{1}{C}\right)^{\frac{\lambda+1}{m}} \tag{29}$$

$$P = \frac{\lambda-m+1}{m} \tag{30}$$

In terms of the slow-roll parameters, the observable quantities measured in the CMB are given by [30].

$$n_s = 1 - 4\varepsilon + \eta \tag{31}$$

$$r = 16\varepsilon \tag{32}$$

Assuming $\phi_{hc} \gg \phi_f$, the horizon crossing value ϕ_{hc} was obtained from (26). The result was substituted into (31) and (32) to analyze the evolution of the scalar spectral index n_s and the tensor-to-scalar ratio r versus the number of e-folds parameter.

In the following, a numerical analysis is performed within the proposed framework, as illustrated in Fig. 2, which presents the variation of the tensor-to-scalar ratio r with the scalar spectral index n_s in the intermediate inflation scenario for three values of the parameter ($m = 0.3, 0.5, 1$). The shaded regions represent the observational constraints from Planck and BICEP, where the inner (green) contour corresponds to the 68% confidence level (CL) and the outer (black) contour corresponds to the 95% CL. The remaining parameters are fixed to $\mathfrak{E} = 20, A = 0.5,\ \lambda = 0.9,\ k = 2, and\ C = 2$. The smaller values of m tend to bring the model predictions closer

to the observationally favored region.

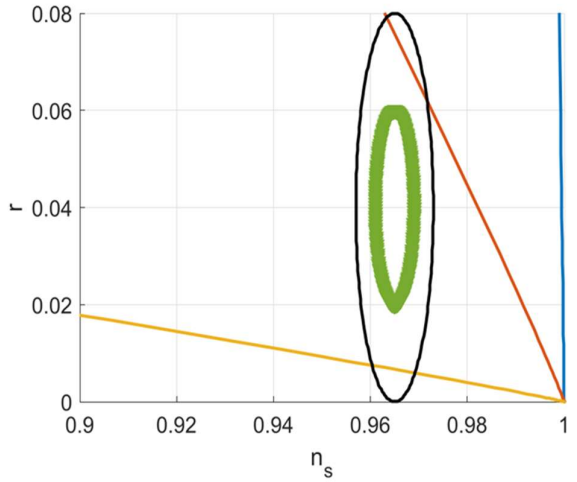

Fig. 2. Tensor-to-Scalar Ratio r versus the Scalar Spectral Index in the Intermediate scenario, shown for three values of the parameter m ($m = 0.3, 0.5, 1$).

IV. Natural Inflation with John and George Models

The natural inflation scenario is examined within the John–George framework. The same methodological approach as in the preceding sections is adopted. The natural inflation potential is taken in the form defined in (33) [22].

$$V(\phi) = \mu^4\left(1 + cos\left(\frac{\phi}{f}\right)\right) \tag{33}$$

In standard natural inflation, the decay constant f must be super-Planckian ($f > M_p$) to satisfy observational constraints. In contrast, in our model with nonminimal derivative coupling, viable inflation can be achieved even for sub-Planckian values of f. This demonstrates that the derivative coupling alleviates the fine-tuning problem present in standard natural inflation.

Using (33), (21), (22), and (25), give (34), (35), and (36), respectively.

$$\varepsilon = -\frac{f}{\mu^4\epsilon\sin\left(\frac{\phi}{f}\right)}\left(1 + \epsilon\mu^4\left(1 + \cos\left(\frac{\phi}{f}\right)\right)\right)\times \left[\epsilon^2\mu^8\frac{1}{f^2}\sin^2\left(\frac{\phi}{f}\right) + \frac{\mu^4}{f^2}\cos\left(\frac{\phi}{f}\right)\left(1 + \epsilon\mu^4\left(1 + \cos\left(\frac{\phi}{f}\right)\right)\right)\right] \tag{34}$$

$$\eta = \frac{2\epsilon^2\left(-\mu^4\frac{1}{f^2}\cos\left(\frac{\phi}{f}\right)\right)\left(1+\epsilon\mu^4\left(1+\cos\left(\frac{\phi}{f}\right)\right)\right)+\epsilon^3\left(-\mu^4\frac{1}{f}\sin\left(\frac{\phi}{f}\right)\right)}{\epsilon^2\left(-\mu^4\frac{1}{f^2}\cos\left(\frac{\phi}{f}\right)-\epsilon^2\mu^8\frac{1}{f^2}\sin^2\left(\frac{\phi}{f}\right)\right)} - \frac{\left(\mu^4\frac{1}{f^3}\sin\left(\frac{\phi}{f}\right)\right)(1+\epsilon\mu^4\left(1+\cos\frac{\phi}{f}\right))^2}{\epsilon^2\left(-\mu^4\frac{1}{f^2}\cos\left(\frac{\phi}{f}\right)-\epsilon^2\mu^8\frac{1}{f^2}\sin^2\left(\frac{\phi}{f}\right)\right)} \tag{34}$$

$$N = \frac{1}{f}\ln\left(\frac{2+\cos\left(\frac{\phi_f}{f}\right)}{2+\cos\left(\frac{\phi_i}{f}\right)}\right) \tag{35}$$

A numerical analysis of the tensor-to-scalar ratio r vs Scalar Spectral Index n_s is performed for the natural inflation scenario, with the slow-roll ϵ taken into account in the following.

Fig. 3 shows the plot of the Tensor-to-Scalar ratio, r versus Scalar Spectral Index n_s in the Natural Inflation scenario with nonminimal derivative coupling, for three values of the decay constant f ($f = 0.5, 1, 5$). The shaded gray regions indicate the observational constraints from Planck and BICEP, with the darker region corresponding to the 68% confidence level (CL) and the lighter region to the 95% CL. The other parameters are fixed to $\mathfrak{E} = 0.1$, $\mu = 0.1, k = 0.5$, and $C = 1.5$. The results indicate that increasing f shifts the predictions toward lower values of r, improving agreement with observational data.

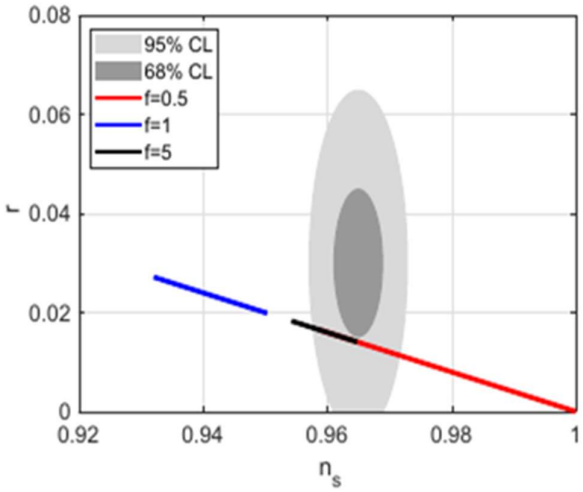

Fig. 3. Tensor-to-Scalar Ratio r versus Scalar Spectral Index in the Natural Inflation scenario with nonminimal derivative coupling, for three values of the decay constant f ($f = 0.5, 1, 5$).

V. Observational Constraints and Discussion

A systematic analysis of the parameter space for both potentials was performed. For intermediate inflation, values of m∼0.5−1 are compatible with Planck observational constraints, while extreme values of the parameters are excluded by observational constraints. For natural inflation with nonminimal derivative coupling, values of the decay constant f that allow for viable inflation even in sub-Planckian regimes were identified, in contrast with standard natural inflation, which requires $f > M_{\mathrm{p}}$. The derivative coupling acts as an additional friction on the scalar field, slowing its evolution and reducing the tensor-to-scalar ratio r, making inflation possible for $f < M_{\mathrm{p}}$. This analysis clearly delineates viable and excluded parameter regions while providing a comparison with the standard model.

The behavior of the tensor-to-scalar ratio r as a function of the scalar spectral index n_s in the framework of intermediate inflation and natural inflation within the nonminimal derivative coupling scenario has been illustrated in Fig. 1 and 2, with the shaded regions corresponding to the observational

constraints at 68% and 95% confidence levels derived from the latest Planck data, respectively.

According to the most recent observational results [31], the scalar spectral index and the tensor-to-scalar ratio are constrained to:

$$n_s = 0.9649 \pm 0.0042, r < 0.056 \quad (37)$$

From Fig. 1, which corresponds to the intermediate inflation case, the trajectories in the (n_s, r) plane for different values of the parameter m is presented. It is observed that the case $m = 0.3$ predicts values of n_s very close to unity, lying outside the observationally preferred region. Therefore, this value of the parameter appears to be disfavored by the Planck constraints.

For the case $m = 0.5$, the predicted trajectory crosses the observational confidence regions and intersects the 95% confidence contour. This indicates that the model becomes compatible with the observational data for this intermediate value of the parameter.

On the other hand, for $m = 1$, the theoretical predictions shift toward smaller values of the tensor-to-scalar ratio, while maintaining values of n_s close to the central observational value. In this case, the predicted points fall well inside the observationally allowed region, showing a better agreement with the Planck constraints.

Similarly, Fig. 2 shows the predictions of the model in the context of natural inflation for different values of the parameter f. The curve corresponding to $f = 0.5$ passes through the allowed observational region and predicts values of n_s and r that are consistent with the Planck constraints.

However, for $f = 1$, the predicted spectral index becomes significantly smaller than the observationally favored value ($n_s \lesssim 0.95$), placing this case outside the confidence regions and thus making it incompatible with the observational data.

For larger values of the parameter, such as $f = 5$, the trajectory approaches the boundary of the observational region and lies close to the 95% confidence contour. This indicates that such values may still be marginally consistent with the observational constraints.

For $N = 60$ e-folds, the model predicts, (38), for intermediate inflation, and (39) for natural inflation, with both values lying within the observational bounds reported by Planck.

$$n_s = 0.96397, r = 0.0019 \quad (38)$$

$$n_s = 0.961176, r = 0.00651 \quad (39)$$

From a physical perspective, the presence of the nonminimal derivative coupling significantly modifies the dynamics of the inflation field. In particular, the derivative coupling enhances the effective gravitational friction acting on the scalar field. As a result, the inflation rolls more slowly along the potential, which suppresses the amplitude of primordial tensor perturbations and consequently reduces the tensor-to-scalar ratio, r.

Therefore, the results obtained from Figs. 1 and 2 indicate that the John–George model with nonminimal derivative coupling can successfully reproduce the observational constraints for specific ranges of the parameters m and f. In particular, intermediate values such as $m \sim 0.5 - 1$ and $f \sim 0.5$ provide the best agreement with the observational data, while other values are disfavored. These results suggest that the considered model provides a viable inflationary scenario consistent with current cosmological observations.

VI. Cosmological Perturbations

Cosmological perturbations of the nonminimal derivative coupling model, commonly referred to as the John–George framework, are considered. Both scalar and tensor fluctuations within the inflationary regime of the model are analyzed. The inflationary parameters arising from perturbations are derived in this context. The same methodological approach as in [28] is employed.

The space-time is decomposed into background and perturbation sectors. The background is described by an isotropic Friedmann–Lemaître–Robertson–Walker (FLRW) metric, while the perturbation sector encodes the anisotropies observed in the CMB. For a consistent treatment of cosmological perturbations in the John–George framework, the action for the curvature perturbation is derived following [32].

$$S^{(2)} = \int dt\, d^3x\, a^3 Q_s \left[\dot{\mathcal{R}}^2 - \frac{c_s^2}{a^2}(\nabla\mathcal{R})^2\right] \quad (40)$$

Where Q_s is the kinetic coefficient of scalar perturbations, determined by the derivatives of the field ϕ and the coupling terms, c_s^2 is the speed of sound squared for scalar perturbations, a is the scale factor and $\mathcal{R}$ is the scalar curvature perturbation. The following expressions, (41) and (42), were obtained.

$$Q_s = \frac{M_p^2}{2}(1 + \epsilon V(\phi))\left[\frac{\dot{\phi}^2}{H^2} + \frac{\gamma\kappa}{H^2}\frac{\dot{\phi}^4}{M_p^2}\right] \quad (41)$$

$$c_s^2 = \frac{1}{1+\gamma\kappa\frac{\dot{\phi}^2}{M_p^2}(1+\epsilon V(\phi))} \quad (42)$$

The differential equation governing $\mathcal{R}$ moving to Fourier space, with the equation of motion for $\mathcal{R}_\kappa$ (comoving perturbation mode) is given by (43), where κ is the wavenumber.

$$\ddot{\mathcal{R}}_k + \left(3H + \frac{\dot{Q}_s}{Q_s}\right)\dot{\mathcal{R}}_k + \frac{c_s^2 k^2}{a^2}\mathcal{R}_k = 0 \quad (43)$$

With the corrected expressions for Q_s and c_s^2, the power spectrum of the comoving curvature perturbations $\mathcal{R}$ in this model can now be determined. The Power spectrum for $\mathcal{R}$ is defined by (44).

$$P_{\mathcal{R}}(k) = \frac{1}{8\pi^2}\frac{H^2}{Q_s c_s^3} \quad (44)$$

which takes the following form of (45).

$$P_{\mathcal{R}}(k) = \frac{H^2}{4\pi^2 M_p^2}\frac{1}{(1+\epsilon V(\phi))\left[\frac{\dot{\phi}^2}{H^2}+\frac{\gamma\kappa}{H^2}\frac{\dot{\phi}^4}{M_p^2}\right]} \cdot [1 + \gamma\kappa\frac{\dot{\phi}^2}{M_p^2}(1 + \epsilon V(\phi))]^{3/2} \quad (45)$$

If $\epsilon \to 0$ (lack of potential coupling), the spectrum returns to a classical dependence modified only by γ. If $\gamma \to 0$, (absence of Einstein tensor coupling), the spectrum is dominated by

$\epsilon V(\phi)$. These two parameters, ϵ and γ, control deviations from the standard canonical model.

The spectral index n_s characterizes the power spectrum dependence of the comoving curvature perturbations $P_{\mathcal{R}}(k)$ as a function of the comoving wavenumber k. It is defined by (46).

$$n_s - 1 = \frac{d\ln P_{\mathcal{R}}}{d\ln k} \tag{46}$$

Comoving wavenumber k is related to the moment of the cosmological horizon aH, with $k = aH$. Consequently:

$$\frac{d\ln k}{dt} = H(1-\epsilon) \tag{47}$$

n_s takes the following form of (48).

$$n_s - 1 = -2\epsilon_H - \frac{\dot{Q}_s}{HQ_s} - 3\frac{\dot{c}_s}{Hc_s} \tag{48}$$

By substituting the expressions of (41) and (42), the spectral index becomes:

$$n_s - 1 = -2\varepsilon - \frac{\frac{\dot{\phi}}{H}\left[2\epsilon+\frac{\dot{\phi}^2}{H^2}(1+4\gamma\kappa)\right]}{(1+\epsilon V(\phi))\left[\frac{\dot{\phi}^2}{H^2}+\frac{\gamma\kappa\,\dot{\phi}^4}{H^2M_p^2}\right]} + \frac{3\gamma\ \frac{\dot{\phi}^2}{M_p^2}}{\left(1+\gamma\kappa\frac{\dot{\phi}^2}{M_p^2}(1+\epsilon\ \ (\phi))\right)} \tag{49}$$

Where ε is given by (21).

The power spectrum of the tensor modes is given by (50).

$$P_T(k) = \frac{2}{\pi^2}\frac{H^2}{M_p^2} \tag{50}$$

The ratio r_s is defined as the ratio of the spectrum of tensor modes to the spectrum of scalar modes:

$$r_s = \frac{P_T(k)}{P_{\mathcal{R}}(k)} \tag{51}$$

Equation (52) was obtained using the previous expressions for $P_T(k)$ and $P_{\mathcal{R}}(k)$.

$$r_s = 8\cdot(1+\gamma\kappa\frac{\dot{\phi}^2}{M_p^2}(1+\epsilon V(\phi)))^{-3/2}\cdot(1+\epsilon V(\phi))\left[\frac{\dot{\phi}^2}{H^2}+\frac{\gamma\kappa}{H^2}\frac{\dot{\phi}^4}{M_p^2}\right] \tag{52}$$

From (17), the expression for $\dot{\phi}$ is obtained. Consequently, (41), (42), (49), and (52) lead to (53), (54), (55), (56), and (57) respectively.

$$Q_s = \frac{M_p^2}{2}(1+\epsilon V(\phi))\left[\frac{(1+\epsilon V(\phi))^2}{\epsilon^2 V'^2(\phi)}+\frac{\gamma\kappa H^2(1+\epsilon V(\phi))^4}{\epsilon^4 V'^4(\phi)M_p^2}\right] \tag{53}$$

$$c_s^2 = \frac{1}{1+\gamma\kappa\frac{\epsilon^2(V'(\phi))^2}{M_p^2H^2(1+\epsilon V(\phi))}} \tag{54}$$

$$P_{\mathcal{R}}(k) = \frac{H^2}{4\pi^2M_p^2}\frac{[1+\gamma\kappa\frac{\epsilon^2(V'(\phi))^2}{M_p^2H^2(1+\epsilon V(\phi))^2}(1+\epsilon V(\phi))]^{3/2}}{(1+\epsilon V(\phi))\left[\frac{\epsilon^2(V'(\phi))^2}{H^2(1+\epsilon V(\phi))^2}+\frac{\gamma\kappa}{H^2}\frac{\epsilon^4(V'(\phi))^4}{M_p^2H^4(1+\epsilon V(\phi))^4}\right]} \tag{55}$$

$$n_s - 1 = -2\varepsilon - \frac{\frac{\epsilon V'(\phi)}{H^2(1+\epsilon V(\phi))}\left[2\epsilon+\frac{\epsilon^2(V'(\phi))^2}{H^4(1+\epsilon V(\phi))^2}(1+4\gamma\kappa)\right]}{(1+\epsilon V(\phi))\left[\frac{\epsilon^2(V'(\phi))^2}{H^4(1+\epsilon V(\phi))^2}+\frac{\gamma\kappa\epsilon^4(V'(\phi))^4}{H^4\ \ M_p^2}\right]} + \frac{3\gamma\kappa\frac{\epsilon^2(V'(\phi))^2}{M_p^2H^4(1+\epsilon V(\phi))^2}}{\left(1+\gamma\kappa\frac{\epsilon^2(V'(\phi))^2}{M_p^2H^4(1+\epsilon V(\phi))^2}(1+\epsilon V(\phi))\right)} \tag{56}$$

$$r = 8(1+\gamma\kappa\frac{\epsilon^2(V'(\phi))^2}{M_p^2H^2(1+\epsilon V(\phi))^2}(1+\epsilon V(\phi)))^{-3/2}\times\left[\frac{(1+\epsilon V(\phi))\epsilon^2(V'(\phi))^2}{H^2(1+\epsilon V(\phi))^2}+\frac{(1+\epsilon V(\phi))\gamma\kappa}{H^2}\frac{\epsilon^4(V'(\phi))^4}{M_p^2H^4(1+\epsilon V(\phi))^4}\right] \tag{57}$$

A. Stability Conditions

The amplitude of the scalar power spectrum is normalized using the observational value measured at the pivot scale $k_* = 0.05\,\mathrm{Mpc}^{-1}$,

$$P_{\mathcal{R}}(k_*) \simeq 2.1\times10^{-9} \tag{58}$$

This normalization provides an additional constraint on the parameters of the model and allows a direct comparison with cosmological observations.

For the physical viability of the inflationary solutions, the scalar perturbations must satisfy the stability condition given by (59).

$$Q_s > 0, c_s^2 > 0 \tag{59}$$

The positivity of Q_s guarantees the absence of ghost instabilities, while $c_s^2 > 0$ ensures that scalar perturbations propagate without gradient instabilities.

Using (53), the kinetic coefficient can be written as

$$Q_s = \frac{M_p^2}{2}(1+\epsilon V(\phi))\left[\frac{(1+\epsilon V(\phi))^2}{\epsilon^2V'^2(\phi)}+\frac{\gamma\kappa H^2(1+\epsilon V(\phi))^4}{\epsilon^4V'^4(\phi)M_p^2}\right] \tag{60}$$

Since $M_p^2 > 0$ and $(1+\epsilon V(\phi)) > 0$ during inflation, the coefficient Q_s remains positive provided that the coupling parameters remain in the physical range considered in our numerical analysis.

Similarly, (61) was obtained from (54).

$$c_s^2 = \frac{1}{1+\gamma\kappa\frac{\epsilon^2(V'(\phi))^2}{M_p^2H^2(1+\epsilon V(\phi))}} \tag{61}$$

The evolution of the kinetic coefficient $Q_s$and the squared sound speed $c_s^2$is presented for both the intermediate inflation potential (Figs. 4 and 5) and the natural inflation potential (Figs. 5 and 6). The results show that the stability conditions $Q_s > 0$and $c_s^2 > 0$are satisfied throughout the inflationary epoch within the nonminimal derivative coupling framework.

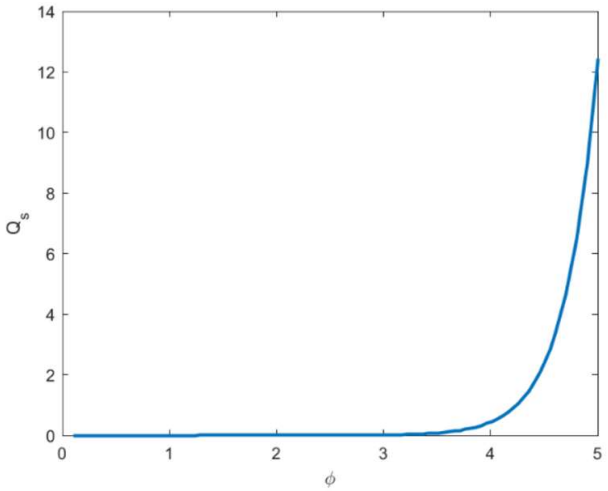

Fig. 4. Evolution of the kinetic coefficient Q_s for the intermediate potential.

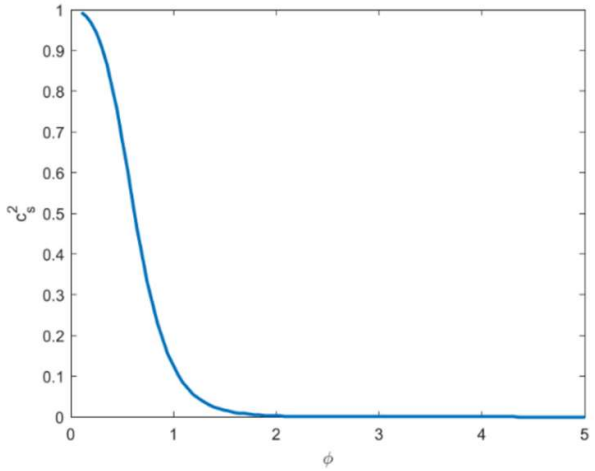

Fig. 5. Evolution of the squared sound speed c_s^2 for the intermediate potential.

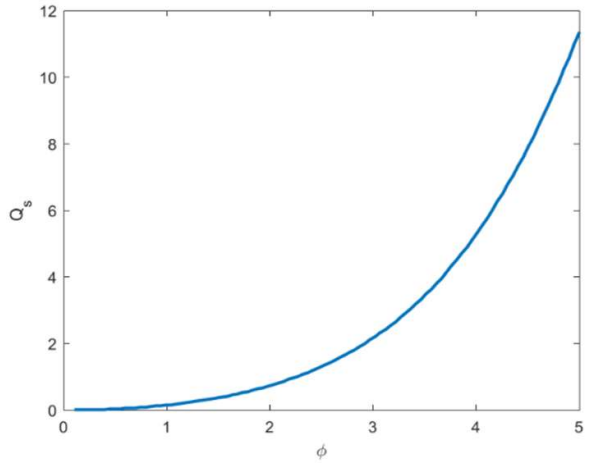

Fig. 6. Evolution of the kinetic coefficient Q_s for the Natural potential.

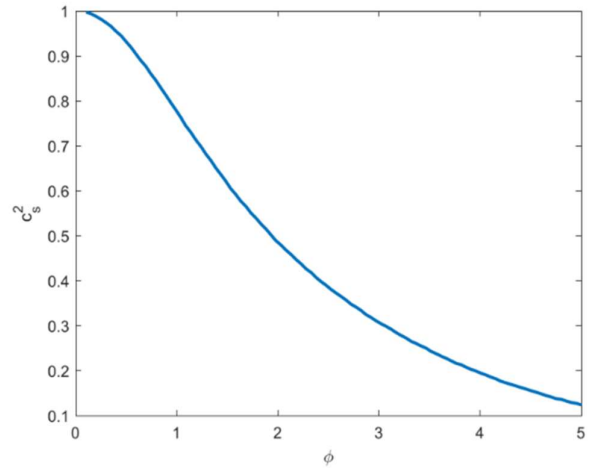

Fig. 7. Evolution of the squared sound speed c_s^2 for the Natural potential.

Therefore c_s^2 remains positive as long as the denominator is positive, which is satisfied for moderate values of the derivative coupling parameter γ. In the parameter region explored in this work, both stability conditions $Q_s > 0$ and $c_s^2 > 0$ are satisfied during the entire inflationary evolution.

For both inflationary scenarios, the stability of scalar perturbations is governed by the behavior of the kinetic coefficient Q_s and the scalar sound speed squared c_s^2. The absence of ghost and gradient instabilities requires $Q_s >$ and $c_s^2 > 0$, respectively.

In the case of intermediate inflation shown in Fig. 4 and Fig. 5, the kinetic coefficient Q_s remains strictly positive throughout the evolution, ensuring a ghost-free configuration. At the same time, the scalar sound speed squared, c_s^2 is positive but rapidly decreases from values close to unity to very small values during inflation. This behavior indicates that scalar perturbations propagate with a reduced effective sound speed.

From a physical perspective, the condition $0 < c_s^2 \leq 1$ guarantees the stability of the system, while the regime $c_s^2 \ll 1$ has important observational consequences. In particular, a low sound speed enhances nonlinear interactions of scalar perturbations, which can lead to a significant level of primordial non-Gaussianities. This suggests that the intermediate inflation scenario within the nonminimal derivative coupling framework may produce observable deviations from Gaussian statistics in the primordial fluctuations.

For the natural inflation scenario, displayed in Fig. 5 and Fig. 6, the kinetic coefficient Q_s also remains positive, confirming the absence of ghost instabilities. The scalar sound speed squared, c_s^2 decreases smoothly during the evolution but remains of order unity over a large range of the scalar field. This indicates that scalar perturbations propagate close to the speed of light.

Consequently, the natural inflation model predicts a standard behavior of perturbations, with suppressed nonlinear effects and negligible non-Gaussianity, consistent with current observational bounds.

Overall, both models are stable at the perturbative level, but they differ significantly in their phenomenology: intermediate inflation is characterized by a reduced sound speed and potentially enhanced non-Gaussian signatures, whereas natural inflation remains closer to the canonical slow-roll regime.

VII. Conclusion

In this study, the scenarios of intermediate inflation and natural inflation are investigated within the framework of a nonminimal derivative coupling model, known as the John–George model. These inflationary scenarios have been extensively studied due to their ability to alleviate the well-known η-problem encountered in many inflationary models.

First, the inflationary potential associated with intermediate inflation is reconstructed by adopting standard conditions commonly used in the literature. Under the slow-roll approximation, the primary inflationary observables, namely the tensor-to-scalar ratio $r$and the scalar spectral index n_s, are derived. A similar analysis is performed for the natural inflation potential, leading to the corresponding inflationary parameters.

For a typical number of e-folds $N = 60$, the resulting values of the inflationary observables are found to be consistent with current cosmological observations. These results indicate that both intermediate and natural inflation can be consistently realized within the John–George framework.

A key feature of this model is the presence of a derivative coupling between the scalar field and the curvature. This coupling enhances the effective gravitational friction acting on the scalar field, thereby slowing the evolution of the inflaton and allowing inflation to proceed even for relatively steep potentials.

Another important consequence of the derivative coupling is the suppression of the tensor-to-scalar ratio r. The enhanced friction reduces the amplitude of primordial gravitational waves, leading to improved agreement between theoretical predictions and observational constraints.

To further support these findings, the perturbative behavior of the inflationary parameters relevant to the model is also examined. The perturbation analysis is carried out in a general form, with the resulting expressions written as functions of the potential $V(\phi)$. A more detailed investigation of the perturbative sector is left for future work.

Overall, the results indicate that both intermediate inflation and natural inflation are viable within the John–George framework. However, the derivative coupling tends to favor regions of parameter space that are consistent with current observational bounds.

Reference

[1] [1] A. H. Guth, “Inflationary universe: A possible solution to the horizon and flatness problems,” Phys. Rev. D, vol. 23, no. 2, pp. 347–356, 1981.

[2] A. Albrecht and P. J. Steinhardt, “Cosmology for grand unified theories with radiatively induced symmetry breaking,” Phys. Rev. Lett., vol. 48, no. 17, pp. 1220–1223, 1982.

[3] A. R. Liddle and D. H. Lyth, Cosmological Inflation and Large-Scale Structure. Cambridge, U.K.: Cambridge Univ. Press, 2000.

[4] J. E. Lidsey et al., “Reconstructing the inflaton potential,” Rev. Mod. Phys., vol. 69, no. 2, pp. 373–410, 1997.

[5] D. H. Lyth and A. R. Liddle, The Primordial Density Perturbation. Cambridge, U.K.: Cambridge Univ. Press, 2009.

[6] J. M. Maldacena, “Non-Gaussian features of primordial fluctuations in single-field inflationary models,” J. High Energy Phys., vol. 2003, no. 05, pp. 013, 2003.

[7] K. Nozari, M. Shoukrani, and B. Fazlpour, “Non-minimal derivative coupling scalar field inflation,” Gen. Relativ. Gravit., vol. 43, pp. 207–220, 2011.

[8] K. Nozari and N. Rashidi, “Braneworld inflation with non-minimal derivative coupling,” Phys. Rev. D, vol. 86, no. 4, pp. 043505, 2012.

[9] P. A. R. Ade et al. (Planck Collaboration), “Planck 2015 results. XX. Constraints on inflation,” Astron. Astrophys., vol. 594, pp. A20, 2016.

[10] K. Nozari and N. Rashidi, “Non-minimal derivative coupling inflationary models in light of observational data,” Adv. High Energy Phys., vol. 2016, pp. 1–16, 2016.

[11] C. Cheung et al., “The effective field theory of inflation,” J. High Energy Phys., vol. 2008, no. 03, pp. 014, 2008.

[12] C. Charmousis, E. J. Copeland, A. Padilla, and P. M. Saffin, “General second-order scalar-tensor theory and self-tuning,” Phys. Rev. Lett., vol. 108, pp. 051101, 2012.

[13] A. Kanfon, G. Edah, and E. Baloitcha, “Intermediate inflation in the framework of modified gravity,” Int. J. Mod. Phys. D, vol. 23, pp. 145008, 2014.

[14] G. W. Horndeski, “Second-order scalar–tensor field equations in a four-dimensional space,” Int. J. Theor. Phys., vol. 10, pp. 363–384, 1974.

[15] L. Amendola, “Cosmology with nonminimal derivative couplings,” Phys. Lett. B, vol. 301, pp. 175–182, 1993.

[16] S. Capozziello and G. Lambiase, “Nonminimal derivative coupling and the recovering of cosmological constant,” Gen. Relativ. Gravit., vol. 31, pp. 1005–1014, 1999.

[17] Y. Akrami et al. (Planck Collaboration), “Planck 2018 results. X. Constraints on inflation,” Astron. Astrophys., vol. 641, pp. A10, 2020.

[18] J. D. Barrow, “Graduated inflationary universes,” Phys. Lett. B, vol. 235, pp. 40–43, 1990.

[19] J. D. Barrow and A. R. Liddle, “Perturbation spectra from intermediate inflation,” Phys. Rev. D, vol. 47, pp. 5219–5223, 1993.

[20] J. D. Barrow and N. J. Nunes, “Dynamics of logamediate inflation,” Phys. Rev. D, vol. 76, pp. 043501, 2007.

[21] K. Rezazadeh et al., “Intermediate inflation in light of Planck data,” J. Cosmol. Astropart. Phys., vol. 2015, no. 09, pp. 053, 2015.

[22] M. Michelotti et al., “Inflationary dynamics with generalized scalar field couplings,” arXiv preprint arXiv:2411.19892, 2024.

[23] K. Freese, J. A. Frieman, and A. V. Olinto, “Natural inflation with pseudo–Nambu–Goldstone bosons,” Phys. Rev. Lett., vol. 65, pp. 3233–3236, 1990.

[24] F. C. Adams et al., “Natural inflation: Particle physics models, power-law spectra for large-scale

structure, and constraints from COBE," Phys. Rev. D, vol. 47, pp. 426–455, 1993.
[25] BICEP/Keck Collaboration, "Improved constraints on primordial gravitational waves using Planck, WMAP, and BICEP/Keck observations through the 2018 observing season," Phys. Rev. Lett., vol. 127, pp. 151301, 2021.
[26] K. Freese and W. H. Kinney, "Natural inflation: Consistency with cosmic microwave background observations of Planck and BICEP2," J. Cosmol. Astropart. Phys., vol. 2015, no. 03, pp. 044, 2015.
[27] P. Goodarzi, "Constraints on inflationary models with nonminimal derivative coupling," arXiv preprint arXiv:2402.06257, 2024.
[28] K. Nozari and N. Rashidi, "Intermediate inflation with nonminimal derivative coupling," Phys. Rev. D, vol. 88, pp. 023519, 2013.
[29] C. Germani and A. Kehagias, "Cosmological perturbations in the new Higgs inflation," J. Cosmol. Astropart. Phys., vol. 2010, no. 05, pp. 019, 2010.
[30] Y. Tiwari, N. Bhaumik, and R. K. Jain, "Understanding large-scale CMB anomalies with the generalized nonminimal derivative coupling during inflation," Phys. Rev. D, vol. 107, pp. 103513, 2023.
[31] I. D. Gialamas et al., "Inflationary phenomenology with generalized scalar couplings," arXiv preprint arXiv:2008.06371, 2020.
[32] Y. Akrami et al. (Planck Collaboration), "Planck 2018 results. I. Overview and the cosmological legacy of Planck," Astron. Astrophys., vol. 634, pp. A61, 2020.